Structure of Ferromagnetic CrAs Epilayers Grown on GaAs(001)

V. H. Etgens,[1,*] P. C. de Camargo,[1,†] M. Eddrief,[1] R. Mattana,[2] J. M. George,[2] and Y. Garreau[3]

[1]*Laboratoire de Minéralogie et de Cristallographie de Paris, CNRS-Universités Paris VI et VII, IPG-P, 4 Place Jussieu, 75252 Paris CEDEX, France*

[2]*Unité Mixte de Physique, CNRS-Thalès, Domaine de Corbeville, and Université Paris-Sud, 91405 Orsay, France*

[3]*LURE, CNRS-CEA-MRES, Bâtiment 209-D BP 34, 91898 Orsay, France*

(Received 8 August 2003; published 23 April 2004)

Magnetic and structural properties of CrAs epilayers grown on GaAs(001) by molecular beam epitaxy have been studied. CrAs epilayers are orthorhombic for all thicknesses investigated but show a structural transition from a metastable phase for very thin films, to the usual bulk MnP-type orthorhombic phase at higher thicknesses. At intermediate thicknesses, there is a predominance of the new phase, although a contribution from the usual CrAs bulk phase remains clearly present. These results strongly suggest that the ferromagnetic signal measured at room temperature comes from the new metastable orthorhombic structure with an expanded **b**-axis induced by the substrate strain.

DOI: 10.1103/PhysRevLett.92.167205 PACS numbers: 75.70.Cn, 61.10.–i, 68.55.Jk, 75.47.Pq

Half-metallic ferromagnets compatible with semiconductor growth and technology are the preferred new materials for spin electronics, because they could lead to a perfect source to inject spin polarized current into a semiconductor.

Shirai [1] first calculated that CrAs with a zinc blende (ZB) structure could be ferromagnetic with a half-metallic electronic band structure. Following his prediction, ferromagnetic behavior was found in CrAs thin films prepared by molecular beam epitaxy (MBE) on GaAs(100) [2]. Zhao [3] extended the search for ferromagnetic materials integrated on GaAs to a very thin CrSb epilayer sandwiched in GaAs. In both cases, ferromagnetism above room temperature was measured, and half-metallic behavior was claimed. In fact, none of the equilibrium phases of bulk CrAs present ferromagnetic order, especially at room temperature. Despite the fact that ZB CrAs is being claimed the cause of this room-temperature ferromagnetism, there is only indirect evidence of the occurrence of this structure [4]. Indeed, the aspects of crystallinity, interface characteristics, and compound formation [3,5] of the CrAs/GaAs system have not yet been systematically investigated.

We have prepared CrAs epilayers by MBE on GaAs(001) and characterized by *in situ* reflection high energy electron diffraction (RHEED), x-ray photoemission spectroscopy (XPS), *ex situ* high resolution transmission electron microscopy (HRTEM), and magnetometry. A set of samples was then studied by grazing incidence x-ray diffraction (GIXD) to determine the crystallographic structure of the CrAs thin epilayers, which turns out to be orthorhombic for all thickness. The constraint imposed by the GaAs substrate on the CrAs and the specific crystalline orientation adopted for the very thin films are assumed to be at the origin of the measured room-temperature ferromagnetism.

While the GaAs substrate has a ZB structure with lattice parameter $a = 5.651$ Å, bulk CrAs displays an orthorhombic MnP structure with lattice parameters (at 295 K) [6]:

$$\mathbf{a}_{\mathrm{CrAs}} = 5.637\ \text{Å}, \qquad \mathbf{b}_{\mathrm{CrAs}} = 3.445\ \text{Å},$$
$$\mathbf{c}_{\mathrm{CrAs}} = 6.197\ \text{Å}.$$

The bulk CrAs magnetic structure corresponds to double-spiral antiferromagnetic order up to 265 K, when it becomes paramagnetic [7,8]. This transition is associated with a discontinuous change of lattice parameters that concerns mainly the $\mathbf{b}_{\mathrm{CrAs}}$ axis which changes by almost 4%. Above 1100 K, the crystal structure evolves to hexagonal NiAs type with Curie-Weiss paramagnetic temperature dependence.

A 100 nm undoped GaAs buffer layer was initially grown on GaAs(001) substrates following standard growth conditions. Following growth, the surface was annealed under As to improve surface flatness. The CrAs was grown at 200 °C with a growth rate of about 8 Å/min under As-rich conditions. The growth starts with the well-ordered GaAs streaky RHEED diagram fading until finally disappearing in a strong diffuse background at 1 Å deposition. After 2 Å, weak streaks appear as elongated spots that do not evolve for thicker films. Annealing under As causes a decrease of the diffuse background at 300 °C, when the diffraction streaks become more elongated and better defined, but still immersed in a diffuse background. No interdiffusion signs could be detected after the survey of core-level photoemission as a function of CrAs thickness. For HRTEM and magnetic measurements, samples have been protected with amorphous ZnSe deposited at low temperature. *Ex situ* HRTEM (Fig. 1) confirms the thickness homogeneity of the CrAs epilayers with abrupt and well-defined interfaces.

The magnetic response of all samples is summarized in Fig. 2, which displays the magnetization as a function of CrAs thickness. Increasing the thickness produces a fast

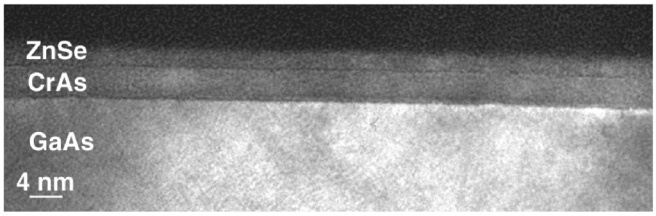

FIG. 1. Transmission electron microscopy picture of the CrAs epilayer of 45 Å on GaAs(001). The zone axis is along the $[1\bar{1}0]$ direction.

decrease of the magnetization, suggesting that the origin of the magnetic signal is limited to a few layers near the interface. The saturation magnetization for 20 Å CrAs corresponds to approximately 1000 emu/cm^3, which gives $\sim 3\mu_B$/Cr for an orthorhombic CrAs, assuming that only chromium atoms contribute to the magnetic moment. These numbers agree with Akinaga [2]; indeed, our results are also comparable for the coercive field and remanent magnetization (inset of Fig. 2). All samples present a hysteretic M-H curve with a clear saturation of magnetization at 5000 Oe and at room temperature.

It is difficult to obtain reliable structural information on these thin epilayers. To address this issue, a custom-made UHV portable chamber has been developed, allowing sample transfer from the MBE facility to a UHV diffraction beam line at the French synchrotron LURE. Thanks to the grazing incidence geometry, we were able to determine the crystal structure of CrAs epilayers, investigated without a protective-capping layer.

The GIXD technique is well adapted for studying the crystallography of very thin films and epilayers [9] because the depth probed by x rays can be strongly reduced

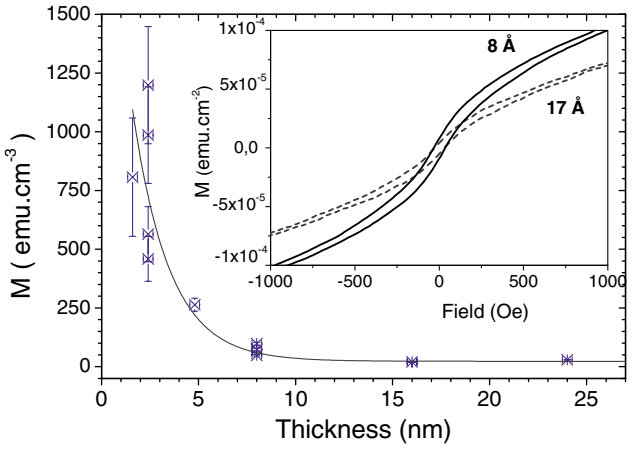

FIG. 2 (color online). Variation of the magnetic moment of CrAs thin film as a function of the thickness. The presence of several points for one given thickness corresponds to different measured samples. The significant spread of values for thin sample is mainly related with the uncertainty in thickness. Hysteresis loops for 8 Å and 17 Å CrAs thickness are shown in the inset. The magnetic field is applied in the plane of the film.

by working close to the critical angle for total reflection of the substrate. In this way, the epilayer signal is enhanced with respect to the bulk signal [10]. Three CrAs samples, namely, X12, X25, and X45, corresponding, respectively, to CrAs thicknesses of 12, 25, and 45 Å, have been transferred under UHV to the GIXD setup. The surface cleanness was verified by Auger spectroscopy, indicating no C and O contamination [11].

The x-ray measurements have been indexed after the cubic GaAs(001) convention for surfaces, expressed in terms of the bulk, with

$$\mathbf{a}^{\mathrm{surf}}_{\mathrm{GaAs}} = 1/2[1\bar{1}0]_{\mathrm{GaAs}}, \qquad \mathbf{b}^{\mathrm{surf}}_{\mathrm{GaAs}} = 1/2[110]_{\mathrm{GaAs}},$$
$$\mathbf{c}^{\mathrm{surf}}_{\mathrm{GaAs}} = [001]_{\mathrm{GaAs}}.$$

Our first search has been for the zinc blende structure observed by Akinaga [2]. Calculations predicted a ZB CrAs lattice of 5.8 Å [12] that corresponds to a 2.6% misfit with GaAs. Both strained and relaxed CrAs epilayers can be detected by the GIXD technique [13]. The search for this structure remained unsuccessful with CrAs epilayers displaying well-defined diffraction peaks, which could be indexed to an orthorhombic structure for all thicknesses. The structure shows two distinct types of epitaxy, one for thin (<20 Å) and another for thick epilayers. A visualization of these findings can be obtained from the surface reciprocal space mapping in Fig. 3.

The first CrAs epitaxy has been determined for the thinnest (X12) epilayer, with the following orientation: $[100]_{\mathrm{CrAs}} \parallel [110]_{\mathrm{GaAs}}$ and $[010]_{\mathrm{CrAs}} \parallel [1\bar{1}0]_{\mathrm{GaAs}}$, with the CrAs **c** axis parallel to the growth direction. This epitaxy displays a theoretical misfit of 6% along $\mathbf{a}_{\mathrm{CrAs}}$ (taking 2 $\mathbf{a}_{\mathrm{CrAs}}$ matching 3 $\mathbf{a}^{\mathrm{surf}}_{\mathrm{GaAs}}$) and 13.9% along $\mathbf{b}_{\mathrm{CrAs}}$. One should stress that only one variant of this epitaxy has been observed reflecting the nonequivalence between the two $\mathbf{a}^{\mathrm{surf}}_{\mathrm{GaAs}}$ and $\mathbf{b}^{\mathrm{surf}}_{\mathrm{GaAs}}$ directions.

A second epitaxy can already be identified for X25 and ends up dominating the diagram for X45 with two variants both with the (**a**,**c**) plane of CrAs lying in the surface plane. The first one has $[100]_{\mathrm{CrAs}} \parallel [100]_{\mathrm{GaAs}}$ and $[001]_{\mathrm{CrAs}} \parallel [010]_{\mathrm{GaAs}}$, and the second $[001]_{\mathrm{CrAs}} \parallel [100]_{\mathrm{GaAs}}$ and $[100]_{\mathrm{CrAs}} \parallel [010]_{\mathrm{GaAs}}$. The $\mathbf{b}_{\mathrm{CrAs}}$ axis remains parallel to the growth direction in both cases. A star has been added in Fig. 3 to differentiate between the two variants of X45. This second epitaxy minimizes the misfit, with a close match between $\mathbf{a}_{\mathrm{CrAs}}$ and $\mathbf{a}_{\mathrm{GaAs}}$ (0.23%), which leaves the orthogonal $\mathbf{c}_{\mathrm{CrAs}}$ axis with a 9.5% misfit. The CrAs lattice parameters measured for this second epitaxy ($\mathbf{b}_{\mathrm{CrAs}}$ included) agree with a fully relaxed epilayer within experimental error.

The epitaxy of the thinner epilayers is more difficult to understand, and is probably related with a metastable phase that nucleates at the very beginning of the growth. The existence of one single variant of this first epitaxy suggests that the nucleation depends on the GaAs surface

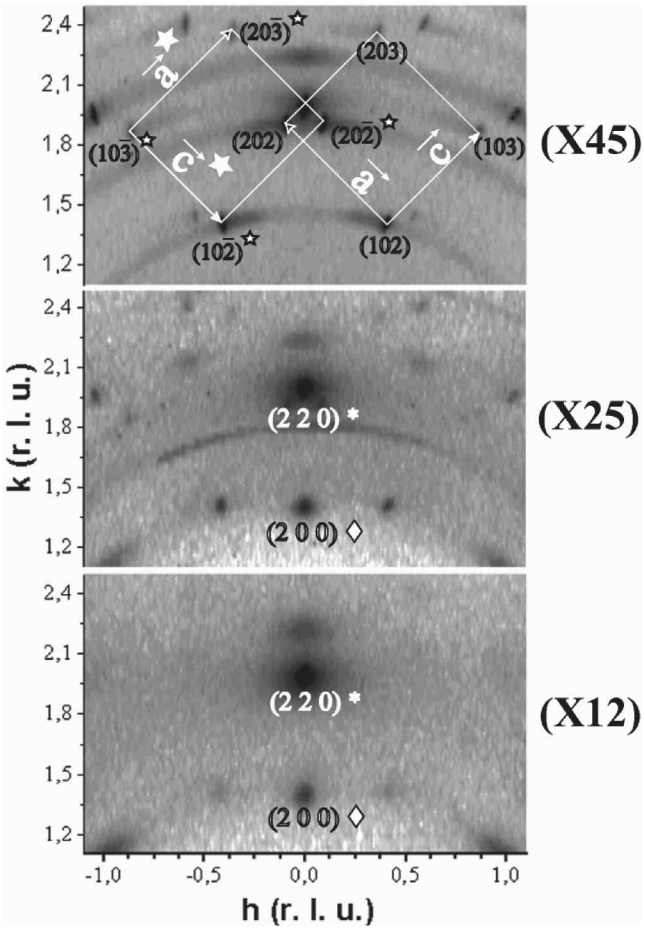

FIG. 3. Partial surface reciprocal space mapping for the CrAs epilayers. The peaks are indexed with respect to bulk, with GaAs represented by a full asterisk and CrAs by a trapeze. For X45, the two different CrAs domains are differentiated by a star in one of the domains.

structure. The dimers and dangling bonds of anions (As) aligned along the $[1\bar{1}0]$ direction produce a strongly asymmetric template [14]. We also measured a significant strain of the $\mathbf{b}_{\mathrm{CrAs}}$ axis that depends on epilayer thickness (Fig. 4).

Weak diffraction rings characteristic of grain dispersion follow the transition from one type of epitaxy to another probably created by the in-plane dispersion of the orientation for different domains and/or domain boundaries.

At this point, the question of the origin of measured magnetic properties for thin epilayers must be reconsidered. The answer should be related, under the light of our experiments, to the orthorhombic first epitaxy observed for thin samples. In fact, one can see in Table I that the $\mathbf{b}_{\mathrm{CrAs}}$ axis of the first epitaxy is significantly expanded relative to bulk CrAs, so that the thinner the epilayer, the larger the expansion along the $\mathbf{b}_{\mathrm{CrAs}}$ axis. In bulk CrAs, it is known that the double-spiral antiferromagnetic-paramagnetic transition is followed by a decrease in the CrAs unit cell volume, mainly due to the large (~4%)

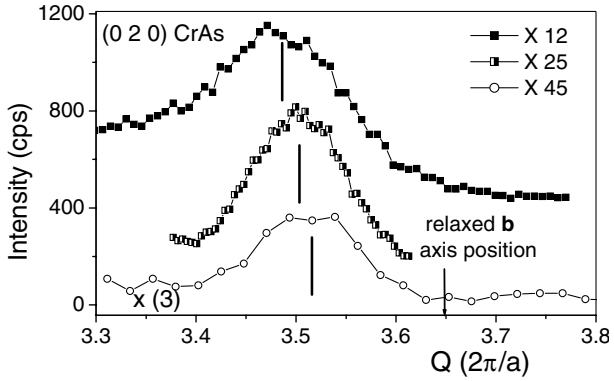

FIG. 4. Radial scan intercepting the (020) peak of CrAs as a function of thickness. The CrAs is under tensile stress which is more pronounced for the thinner epilayer. The arrow indicates the value corresponding to the bulk relaxed value.

spontaneous contraction of the **b** axis [15], as opposed to a smaller increase of both **a** and **c** axes.

In order to discuss the magnetic order in CrAs/GaAs, it is worth considering its origin. Interfacial reactions forming peculiar magnetic compounds or the diffusion of Cr into the GaAs are ruled out because both XPS and HRTEM show a sharp interface. Furthermore, a larger magnetization was always obtained when the substrate was kept at the lowest temperature, during and after growth. Therefore, our GIXD results clearly suggest the strained orthorhombic CrAs (epitaxy 1) or perhaps a new metastable orthorhombic phase, as the origin of the ferromagnetic signal. We provide plausibility arguments to support this conclusion and to motivate theoretical calculations to test these ideas.

Since the pioneer work of Selte *et al.* [8], there is an agreement that CrAs presents an MnP-type orthorhombic structure, with a double-spiral antiferromagnetic spin structure along the **c** axis, coupled to each other in the **ab** plane with an angular displacement of 73.4°.

It is well known that CrAs magnetism is strongly affected substituting Cr by other $3d$ transition metals such as Ti, V, Mn, Fe, Co, and Ni [15] or replacing As by P, Sb, or S [16]. Considering several of these compounds, Suzuki [16] built an interesting phase diagram of the Néel temperature as a function of the **b**-axis lattice parameter, where the most sensitive **b**-axis spacing is varied by replacing Cr or As atoms. This phase diagram clearly indicates a critical smallest **b** size ($\mathbf{b}_{\mathbf{c}} = 3.38$ Å), above which the MnP-type, antiferrohelimagnetic order occurs and also the boundary above which a paramagnetic Curie-Weiss NiAs-type order exists. For the $\mathrm{CrAs}_{1-x}\mathrm{Sb}_x$ system, the Curie-Weiss temperature dependence allows one to obtain local magnetic moments of about $3\mu_B$/Cr atom.

Understanding the microscopic origin of a ferromagnetic phase in CrAs thin films is not an easy task, and will certainly require calculations to determine the contributions from electronic band structure features or from

TABLE I. Lattice parameters of GaAs and CrAs (first epitaxy) along the relevant directions. Note the measured lattice parameter and the remaining strain, showing that the CrAs **b** axis is strongly deformed for thinner epilayers.

GaAs (Å)	CrAs (Å)	X12 Å	X25 Å	X45 Å
$[110] = 3.996$	$\mathbf{a} = 5.637$	5.74 (+0.8%)	5.68 (+0.7%)	···
$[1\bar{1}0] = 3.996$	$\mathbf{b} = 3.445$	3.63 (+5.6%)	3.59 (+4.2%)	3.57 (+3.7%)
$[001] = 5.651$	$\mathbf{c} = 6.197$	6.15 (−0.7%)	6.21 (+0.2%)	···

the localized magnetic ion interactions. MnAs and $Cr_{1-x}Mn_xAs$ both show ferromagnetic exchange coupling, even for the MnP structure, while for $Cr_{1-x}V_xAs$ with $x \geq 0.05$ helimagnetic ordering is destroyed, strongly supporting the idea that the *d*-band features are relevant to the magnetic ordering. In this case, the ferromagnetism should appear by taking into account the distortions of the Fermi surface, mainly due to the expansion along the **b** axis.

On the other hand, the experimental evidence of electronic and thickness effects, combined with the results of Fig. 1 and the data in Table I, suggests that the exchange interaction of localized 3*d* states may contribute to the stabilization mechanism of a ferromagnetic phase. Finally, a subtle proportion of localized and band effects can be the origin of the stabilization of the new orthorhombic ferromagnetic phase at room temperature in the CrAs/GaAs system.

As for the CrAs/GaAs heterostructure, it is worth stressing that, from the crystallographic point of view, no evidence of a ZB CrAs structure could be found, neither with GIXD nor observing the RHEED diagram, in contrast with reports from Akinaga [2] and Okazama [17].

The magnetic and structural properties of CrAs epilayers grown by MBE on GaAs(001) have been measured. The structure of very thin CrAs epilayers was determined by GIXD. It turns out that, even for the thinnest sample (12 Å), CrAs is orthorhombic, although it shows a transition in the epitaxial orientation around a thickness of 20 Å. We suggest that the ferromagnetic signal measured at room temperature comes from a new metastable orthorhombic structure, corresponding to an expansion of 5.6% along the CrAs **b** axis for the 12 Å film, with decreasing strain for the thicker samples (Table I). This strain is very large to be accommodated elastically, so we propose the formation of a new ferromagnetic phase in the first few epilayers.

Given the above considerations, it is clear that the transition from the first to the second epitaxy is progressive as a function of the epilayer thickness, and the residual ferromagnetic signal is associated with the orthorhombic ferromagnetic phase persisting near the CrAs/GaAs interface. In this case, the CrAs/GaAs system may have two orthorhombic growth regimes, with different lattice parameters, where the largest difference is in the orientation and strain of the **b** axis.

We are indebted to D. Demaille, A. Fert, N. Mattoso, and D. Mosca for enlightening discussions and for support of French Program Action Concertée Nanosciences-Nanotechologies. P. C. de Camargo acknowledges financial support from CNPq.

*Author to whom correspondence should be addressed. Electronic address: victor.etgens@lmcp.jussieu.fr

†P. C. de Camargo is on leave from Departamento de Física-UFPR, 81531-990 Curitiba PR, Brazil.

[1] M. Shirai, Physica (Amsterdam) **10E**, 143 (2001).
[2] H. Akinaga, T. Manago, and M. Shirai, Jpn. J. Appl. Phys. **39**, 1118 (2000).
[3] J. H. Zhao, F. Matsukura, K. Takamura, E. Abe, D. Chiba, and H. Ohno, Appl. Phys. Lett. **79**, 2776 (2001).
[4] H. Ofuchi, M. Mizuguchi, K. Ono, M. Oshima, H. Akinaga, and T. Manago, Nucl. Instrum. Methods **199**, 227 (2003).
[5] J. R. Waldrop and R. W. Grant, Appl. Phys. Lett. **34**, 630 (1979).
[6] H. Boller and A. Kallel, Solid State Commun. **9**, 1699 (1971).
[7] T. Suzuki and H. Ido, J. Appl. Phys. **79**, 5224 (1996).
[8] K. Selte, A. Kjekshus, W. E. Jamison, A. F. Andresen, and J. E. Engebretsen, Acta Chem. Scand. **25**, 1703 (1971).
[9] I. K. Robinson, in *Handbook of Synchrotron Radiation* (North-Holland, Amsterdam, 1991), Vol. 3.
[10] V. H. Etgens, M. Sauvage-Simkin, R. Pinchaux, J. Massies, N. Jedrecy, A. Waldhauer, S. Tatarenko, and P. H. Jouneau, Phys. Rev. B **47**, 10 607 (1993).
[11] It is worth noticing that the UHV transferring device has being successfully tested in previous studies of photoemission: M. Eddrief, R. Mattana, M. Marangolo, G.-M. Guichar, V. H. Etgens, D. H. Mosca, and F. Sirotti, Appl. Phys. Lett. **81**, 4553 (2002).
[12] I. Galanakis, Phys. Rev. B **66**, 012406 (2002).
[13] A. A. Williams *et al.*, Phys. Rev. B **43**, 5001 (1991).
[14] T. Hashisume, Q. K. Xue, A. Ichimiya, and T. Sakurai, Phys. Rev. Lett. **73**, 2208 (1995).
[15] T. Suzuki and H. Ido, J. Appl. Phys. **69**, 4624 (1991).
[16] T. Suzuki and H. Ido, J. Appl. Phys. **73**, 5686 (1993).
[17] D. Okazawa, K. Yamamoto, A. Nagashima, and J. Yoshino, Physica (Amsterdam) **10E**, 229 (2001).